HHS Public Access

Author manuscript

*Acta Neuropathol*. Author manuscript; available in PMC 2018 July 01.

Published in final edited form as:

*Acta Neuropathol*. 2017 July ; 134(1): 35–44. doi:10.1007/s00401-017-1734-6.

# Bystander mechanism for complement-initiated early oligodendrocyte injury in neuromyelitis optica

**Lukmanee Tradtrantip**, **Xiaoming Yao**, **Tao Su**, **Alex J. Smith**, and **Alan S. Verkman**

Departments of Medicine and Physiology, University of California, San Francisco, CA

## Abstract

Neuromyelitis optica spectrum disorder (herein called NMO) is an autoimmune inflammatory disease of the central nervous system in which immunoglobulin G antibodies against astrocyte water channel aquaporin-4 (AQP4-IgG) cause demyelination and neurological deficit. Injury to oligodendrocytes, which do not express AQP4, links the initiating pathogenic event of AQP4-IgG binding to astrocyte AQP4 to demyelination. Here, we report evidence for a complement 'bystander mechanism' to account for early oligodendrocyte injury in NMO in which activated, soluble complement proteins following AQP4-IgG binding to astrocyte AQP4 result in deposition of the complement membrane attack complex (MAC) on nearby oligodendrocytes. Primary cocultures of rat astrocytes and mature oligodendrocytes exposed to AQP4-IgG and complement showed early death of oligodendrocytes in close contact with astrocytes, which was not seen in pure oligodendrocyte cultures, in cocultures exposed to AQP4-IgG and C6-depleted serum, or when astrocytes were damaged by a complement-independent mechanism. Astrocyte-oligodendrocyte cocultures exposed to AQP4-IgG and complement showed prominent MAC deposition on oligodendrocytes in contact with astrocytes, whereas C1q, the initiating protein in the classical complement pathway, and C3d, a component of the alternative complement pathway, were deposited only on astrocytes. Early oligodendrocyte injury with MAC deposition was also found in rat brain following intracerebral injection of AQP4-IgG, complement and a fixable dead-cell stain. These results support a novel complement bystander mechanism for early oligodendrocyte injury and demyelination in NMO.

### Keywords

NMO; aquaporin-4; astrocyte; oligodendrocyte; complement-dependent cytotoxicity

## Introduction

Neuromyelitis optica spectrum disorders (herein called NMO) is an autoimmune disease of the central nervous system in which circulating immunoglobulin G autoantibodies against astrocyte water channel aquaporin-4 (AQP4-IgG) found in most NMO patients can produce injury to spinal cord, optic nerve and brain [13]. AQP4-IgG binding to AQP4 on astrocytes

Address correspondence to: Alan S. Verkman, M.D., Ph.D., 1246 Health Sciences East Tower, University of California, San Francisco, CA 94143-0521, U.S.A.; Phone: (415) 476-8530; Fax: (415) 665-3847; Alan.Verkman@ucsf.edu; http:/www.ucsf.edu/verklab.

**Competing interests.** None of the authors has competing interests.

is likely the major initiating pathogenic event in AQP4-IgG seropositive NMO, which causes downstream inflammation, activation of complement- and cell-mediated cytotoxicity mechanisms, blood-brain barrier disruption, demyelination and neuronal injury. Pathology in humans and animal models indicates that oligodendrocyte injury and demyelination are early and prominent features in NMO [12, 19].

Activation of the classical complement pathway is a central mechanism in NMO pathogenesis. There is prominent perivascular deposition of the complement membrane attack complex (MAC) in human NMO lesions [14, 16, 24] and complement-dependent NMO pathology is seen in rodents administered AQP4-IgG [1, 2, 26]. Astrocyte injury caused by MAC deposition is a consequence of AQP4-IgG binding to astrocyte AQP4 and subsequent complement activation initiated by C1q binding to astrocyte-bound AQP4-IgG. However, oligodendrocytes, whose injury triggers demyelination, do not express AQP4 and hence cannot bind AQP4-IgG. It has been postulated that oligodendrocyte injury and demyelination in NMO is a secondary action of the inflammatory process and astrocyte loss, or perhaps caused by inflammatory or other factors such as excitatory neurotransmitters released by injured astrocytes [15].

Here, we report evidence for a complement ‘bystander mechanism’ for early oligodendrocyte injury and demyelination in NMO in which activated, soluble complement components (C5b67) produced in response AQP4-IgG binding to astrocytes and activation of the classical complement pathway result in MAC deposition on nearby oligodendrocytes and consequent injury. Oligodendrocytes are particularly susceptible to complement injury because of their low expression of CD59 [21, 28, 37], a membrane-bound glycoprotein that inhibits MAC formation. It has been estimated that the range for bystander-induced complement cytotoxicity is ~2.5 μm [8], which would allow injury of closely intermingled oligodendrocytes following complement activation on astrocytes. There is precedent for complement bystander cytotoxicity for astrocyte injury in Rasmussen’s encephalitis following complement activation by glutamate receptor GluR3 autoantibodies in neurons [36], and for a large increase in membrane conductance of rat cerebral artery smooth-muscle cells caused by complement activation on aged erythrocytes [18]. The experimental evidence here includes cytotoxicity and immunofluorescence in astrocyte-oligodendrocyte cocultures exposed to AQP4-IgG and complement, as well as in rat brain following intracerebral AQP4-IgG administration.

## Materials and methods

### Materials

Recombinant purified AQP4-IgG (rAb-53) [3, 6] was provided by Dr. Jeffrey Bennett (University of Colorado, Aurora CO). Chemicals were purchased from Sigma-Aldrich (St. Louis, MO) unless specified otherwise. Sprague-Dawley rats were purchased from Charles River Laboratories (Wilmington, MA) and bred at UCSF. AQP4$^{-/-}$ rats for control studies were generated by CRISPR/Cas9 as will be reported separately. All animal procedures were approved by the University of California, San Francisco Animal Care and Use Committee (IACUC).

## Cell culture

Oligodendrocyte precursor cell (OPC) cultures from rat brain were generated as described [7, 40]. Briefly, brains from postnatal day 7 pups were harvested and cortex was placed in cold Hank's balanced salt solution (HBSS, pH 7.2; Invitrogen, Camarillo, CA) without $Ca^{2+}$ and $Mg^{2+}$. After removal of the meninges, tissue was diced, digested in papain and DNase I, triturated with an 18-gauge needle, and centrifuged. The tissue pellet was resuspended in DMEM containing 10 % FBS and trypsin inhibitor, passed through a 70-μm nylon strainer and centrifuged on 15 % Percoll. OPCs were enriched using anti-O4 MicroBeads (Miltenyi Biotec, San Diego, CA). Cells were cultured in NeuroBasal medium (Gibco, Grand Island, NY) containing 1 % FBS, 2 % B27-supplement without vitamin A, non-essential amino acids, L-glutamine and platelet-derived growth factor-AA (25 ng/ml; ProSpec-Tany TechnoGene, Rehovot, Israel) for 24 h and then in the same medium without serum. The OPC yield was $5 \times 10^5$ cells per brain with > 95% purity. Rat brain astrocytes were isolated using the same steps as used for OPCs but concentrated by using anti-GLAST MicroBeads (Miltenyi Biotec, San Diego, CA) and cultured in DMEM/F12 with 10% FBS. Cocultures containing OPCs and astrocytes were generated to give ~ 10 to 1 cell ratio. After isolation, cells were cultured in PDL-coated flasks with medium consisting of Advanced DMEM/F12 (Gibco) containing B27, 4 mM glutamine, 25 ng/ml PDGFaa and 0.75% FBS. Passage 3 cells were sub-cultured (20,000 cells/well) on PDL-coated 18-mm diameter round coverglasses (Neuvitro, Vancouver, WA) in 12-well plates. After 24 to 48 h in culture, when cells reached 50–60 % confluent, 150 nM triiodothyronine (T3) was added to the medium with reduced PDGF (5 ng/ml) to induce the OPC maturation. Cells were cultured for 3 more days, with medium (containing T3) changed once.

## Complement-dependent cytotoxicity

Specified concentrations of AQP4-IgG (or control human IgG, Thermo Fisher Scientific, Rockford, IL) and human complement (Innovative Research, Novi, MI) were added in Hank's buffer, and cells were incubated at 37°C for specified times. A fixable dead-cell stain (amine-reactive dye, Invitrogen, Eugene, OR) at 1:1000 dilution was added 30 min prior to cell fixation. In some experiments C6-deficient human complement, without or with added C6 (64 μg/ml) (both from Complement Technology, Tyler, TX) to rescue complement activity, was used instead of normal complement. In some experiments the astrocyte toxin α-aminoadipic acid (Santa Cruz Biotechnology, Dallas, TX) at 2 mM was added to astrocyte-oligodendrocyte cocultures for 75 min.

For live-cell real-time imaging, astrocyte-oligodendrocyte cocultures were grown on 6-well plates and imaged by phase-contrast optics using a 20×, 0.45 NA objective lens on a Nikon Eclipse Ti microscope equipped with an environmental chamber at 37°C and 5% $CO_2$. Ethidium homodimer-1 (1 μM, Invitrogen, Eugene, OR) was added to the culture medium prior to image acquisition. Transmitted light (phase-contrast) and red fluorescence images were obtained sequentially every 2 min for a 30 min baseline period and then for a further 2 hours following addition of 20 μg/ml AQP4-IgG and 2% complement.

### Rat studies

AQP4-IgG was delivered to adult rats by intracerebral injection. Rats were anesthetized with ketamine (100 mg/kg) and xylazine (10 mg/kg) and mounted on a stereotaxic frame. Following a midline scalp incision a 1-mm diameter burr hole was drilled 0.5 mm anterior and 3.5 mm lateral to the bregma for insertion of a 40-μm diameter tip pulled glass pipette to a depth of 3 mm. AQP4-IgG (or control IgG, each 15 μg) together with 26% complement and 6 μM fixable dead cell dye ethidium homodimer-1 (EH-1) was infused in a volume of 6 μL over 9 min. The glass pipette was kept in place for 10 min before withdrawal to prevent leaking. At 90 min rats were deeply anesthetized and transcardiacally perfused with 200 mL heparinized PBS and 200 mL of 4 % PFA in PBS. Brains were removed and post-fixed for 4 h in 4 % PFA and cryoprotected in 20 % sucrose for cutting 7-μm thick sections on a cryostat.

### Immunofluorescence

Following treatments, cell cultures were rinsed in PBS, fixed with 4% PFA for 15 min, and then were blocked with 1% BSA and 0.2% Triton-X in PBS for 1 hour. Cultures were incubated at room temperature for 2 h, and brain sections were incubated at 4 °C overnight with antibodies against AQP4 (1:200, Santa Cruz Biotechnology), GFAP (glial fibrillary acidic protein, 1:1000; Millipore), MBP (myelin basic protein, 1:100, Santa Cruz Biotechnology), Olig2 (oligodendrocyte lineage transcription factor 2, 1:100, Santa Cruz Biotechnology), C1q-FITC (1:50, Abcam, Cambridge, MA), C5b-9 (1:100, Santa Cruz Biotechnology), C3d (1:50, Santa Cruz Biotechnology) or CD59 (5 μg/mL, Lifespan Bioscience), followed by the appropriate species-specific Alexa Fluor-conjugated secondary antibody for 1 h (5 μg/mL each, Invitrogen). AQP4-IgG was detected using Alexa Fluor-conjugated anti-human IgG. Sections were mounted with VectaShield (Vector Laboratories, Burlingame, CA) and immunofluorescence was visualized on a Nikon confocal microscope using a 20×/0.5 N.A., 60×/1.42 N.A. oil objective lens or 100×/1.25 N.A. oil objective lens.

## Results

### Characterization of rat astrocyte-oligodendrocyte cocultures

Rat astrocyte-oligodendrocyte cocultures were used for the in vitro studies here because, unlike brain slices or intact brain, the extracellular solution composition and cellular makeup can be specified with precision, and high-resolution imaging is possible. For studies of astrocyte-related oligodendrocyte injury, culture conditions were established to give a ratio of oligodendrocytes : astrocytes of ~10:1 in order to visualize several oligodendrocytes surrounding well-separated astrocytes. Fig. 1a shows astrocyte-oligodendrocyte cocultures with different cell ratios. The various cocultures were >95% pure, as seen by immunofluorescence for markers of astrocytes (GFAP), mature oligodendrocytes (MBP) and immature oligodendrocytes (NG2).

The cocultures showed expression of AQP4, the target of AQP4-IgG autoantibodies, on astrocytes but not oligodendrocytes. The cocultures expressed complement inhibitor protein CD59 on astrocytes but not oligodendrocytes (Fig. 1b), in agreement with prior findings [21, 37], predicting much greater intrinsic susceptibility of oligodendrocytes than astrocytes to

complement-mediated cytotoxicity (CDC). Functional CDC studies were done by measurement of cell death following exposure to AQP4-IgG and human complement. In pure cell cultures, AQP4-IgG and control-IgG produced similar low oligodendrocyte cytotoxicity, whereas substantially greater cytotoxicity was seen for AQP4-IgG vs. control-IgG in the astrocyte cultures (Fig. 1c).

### Complement bystander mechanism for oligodendrocyte injury in astrocyte cocultures

CDC measurements done in astrocyte-oligodendrocyte cocultures showed killing of MBP-positive (mature, myelinating) oligodendrocytes located nearby astrocytes. Time-lapse imaging, as seen in Supplemental Movie 1 with still images shown in Fig. 2a, showed that an early event following AQP4-IgG and complement exposure is slight swelling and structural alterations of astrocytes, with retraction of oligodendrocyte processes that are in contact with astrocytes, followed by eventual oligodendrocyte death as seen by uptake of red fluorescing ethidium homodimer-1. The example here shows that complement can cause oligodendrocyte death even under conditions where the adjacent astrocyte survives, demonstrating the high sensitivity of cultured oligodendrocytes to complement-mediated injury, due in part to the absence of CD59. Many examples were also seen of dead oligodendrocytes near dead astrocytes (not shown).

Quantitative data for oligodendrocyte killing were obtained following incubation of cocultures for 2 hours with AQP4-IgG and complement, followed by fixation, immunostaining and fluorescence imaging. Fig. 2b shows red (dead cell) staining of many oligodendrocytes (labeled blue with MBP antibody) near astrocytes (labeled green with GFAP antibody). Fig. 2c summarizes the percentage of dead oligodendrocytes located at different distances from astrocytes, showing marked, preferential killing of nearby oligodendrocytes.

Further experiments tested the hypothesis that killing of oligodendrocytes nearby astrocytes occurs by a complement bystander mechanism. Immunofluorescence was done to determine the cellular deposition pattern of the initiating complement component C1q and the terminal complement membrane attack complex C5b-9. Fluorescence micrographs in Fig. 3a–b, as quantified in Fig. 3c, show that C1q immunofluorescence is restricted to astrocytes when cells were exposed to AQP4-IgG and complement, whereas C5b-9 immunofluorescence is seen on both astrocytes and nearby oligodendrocytes. Also, C3d (the degradation product of C3b) immunofluorescence was restricted to astrocytes (Fig. 3d), providing evidence against involvement of the alternative complement pathway in oligodendrocyte injury. These findings demonstrate that activation of the classical complement pathway in response to AQP4-IgG binding to AQP4 occurs exclusively on astrocytes, whereas the terminal complement membrane attack complex is deposited as well on nearby oligodendrocytes as would be predicted for a bystander mechanism.

To investigate the possibility that oligodendrocyte killing might be caused by early components of the complement pathway (C1 though C5) such as anaphylotoxins C3a and C5a, which are activated upon AQP4-IgG binding to astrocytes, astrocyte-oligodendrocyte cocultures were exposed to C6-depleted human serum in which activation of the classical complement pathway can occur but the terminal attack complex cannot form. Exposure of

cocultures to C6-depleted serum did not produce cytotoxicity under conditions in which marked cell killing was seen with normal (complement-containing) serum (Fig. 4a, c), supporting the conclusion that MAC deposition on oligodendrocytes mediates cell death. As a control, addition of purified C6 to the C6-depleted serum restored cell killing, confirming the activity of the C6-depleted serum.

### Oligodendrocyte responses to complement-independent astrocyte injury

To determine if astrocyte damage by itself is sufficient to injure nearby oligodendrocytes, astrocytes were injured by a complement-independent mechanism using the astrocyte-selective toxin α-aminoadipic acid [5, 11]. The time and concentration for toxin administration were first established in which many astrocytes but few oligodendrocytes were killed in pure cultures. Exposure of astrocyte cultures to 2 mM α-aminoadipic for 75 min caused 82% cell death in pure astrocyte cultures but only 8% death in pure oligodendrocyte cultures. Under these coculture conditions there was marked astrocyte cytotoxicity but little oligodendrocyte death (Fig. 4b–c). These results suggest that effector molecules produced by injured astrocytes, such as excitatory neurotransmitters or cytokines, do not injure nearby oligodendrocytes under the in vitro culture conditions here.

### Evidence for a complement bystander mechanism in rat brain in vivo

Last, experiments were done to support a complement bystander mechanism for oligodendrocyte injury in rat brain in vivo. For these studies we adapted an intracerebral injection model in rats in which AQP4-IgG injection into brain produces characteristic NMO pathology with astrocytopathy, complement activation, inflammation and demyelination [1]. To study early cell death, rat brains were injected with AQP4-IgG, human complement, and the dead cell stain ethidium homodimer-1 (EH-1) used in time-lapse imaging studies (Fig. 5a). Complement was included with the injected AQP4-IgG in these studies to ensure immediate and consistent exposure of astrocytes to complement for examination of fixed brain sections. Brains were examined at an early (90 min) time point and a dead cell stain was included to enable visualization of injured oligodendrocytes prior to their disappearance.

Fig. 5b shows many EH-1 positive dead cells following AQP4-IgG injection in $AQP4^{+/+}$ rat brain, but not in $AQP4^{+/+}$ rat brain following control-IgG injection or in $AQP4^{-/-}$ rat brain following AQP4-IgG injection. At higher magnification, EH-1 positive astrocytes and nearby oligodendrocytes were seen 90 min after AQP4-IgG injection in $AQP4^{+/+}$ rat brain (Fig. 5c), which was not seen in $AQP4^{+/+}$ rat brain injected with control-IgG injection or in $AQP4^{-/-}$ rat brain injected with AQP4-IgG (Fig. 5d). Injected human AQP4-IgG (detected with anti-human secondary antibody) was seen on EH-1 positive cells and colocalized with C5b-9 (Fig. 5e, row i). C5b-9 positive, EH-1 positive cells include both astrocytes (row ii) and oligodendrocytes (row iii). Quantitation showed 1.8 ± 0.3-fold greater MAC deposition (C5b-9 staining) on GFAP-positive cells than on Olig2-positive cells (3 rats, 5 contiguous sections analyzed per rat). The results support the conclusion that AQP4-IgG and complement injures AQP4-expressing astrocytes and nearby oligodendrocytes in rat brain by a complement bystander mechanism.

## Discussion

The data here support a novel pathogenesis mechanism in AQP4-IgG seropositive NMO that could explain the early and marked oligodendrocyte injury and demyelination. The generally accepted pathogenesis mechanism in seropositive NMO involves AQP4-IgG entry into the central nervous system and binding to astrocyte AQP4, which causes primary complement- and cell-mediated astrocyte injury with secondary inflammation, blood-brain barrier disruption, and demyelination [17]. The involvement of AQP4-sensitized T cells has also been proposed based on CNS pathology following T cell administration [4, 27], though the relevance of non-humoral mechanisms in human NMO is unclear. Various alternative NMO pathogenesis mechanisms have been proposed [9, 10] but largely refuted [23, 25], including excitotoxic injury, AQP4-IgG inhibition of AQP4 water permeability, and AQP4-IgG-induced internalization of specific AQP4 isoforms. The substantially greater intrinsic sensitivity of oligodendrocytes to complement-induced injury compared to that of astrocytes would amplify complement bystander effects. Of note, other complement regulatory proteins such as CD46 and CD55 cannot protect against bystander cytotoxicity because they target steps in the complement activation pathway upstream of C6 activation [41].

Several lines of evidence support a complement bystander mechanism for oligodendrocyte injury following activation of the classical complement pathway by AQP4-IgG binding to AQP4 on astrocytes (Fig. 6), in which the soluble C5b67 complex that is formed on astrocytes diffuses to nearby oligodendrocytes. Killing by AQP4-IgG and complement was seen in oligodendrocytes very near astrocytes in cocultures; AQP4-IgG-induced killing was not seen pure oligodendrocyte cultures, as expected, as oligodendrocytes do not express AQP4. The deposition of C1q and C3d exclusively on astrocytes, and the deposition of MAC on both astrocytes and nearby oligodendrocytes, provides strong support that complement activation is initiated by astrocytes, resulting in MAC deposition and killing of astrocytes and nearby oligodendrocytes. The absence of cytotoxicity with C6-depleted serum indicates that oligodendrocyte killing is caused by the terminal membrane attack complex rather than upstream components of complement activation, such as anaphylatoxins, that are produced following AQP-IgG-induced activation of the classical complement pathway. The absence of oligodendrocyte death in response to astrocyte death produced by α-aminoadipic acid suggests little contribution of complement-independent oligodendrocyte injury mechanisms in the cocultures, which is supported by AQP4-IgG / complement studies where oligodendrocyte death is seen nearby viable astrocyte. The substantially greater intrinsic sensitivity of oligodendrocytes to complement-induced injury compared to that of astrocytes, because of differential CD59 expression, amplifies the complement bystander effect.

Complement deposition occurs most efficiently when AQP4 is aggregated into orthogonal arrays [20]. AQP4 arrays are concentrated at specific subcellular sites in vivo [29, 38], most notably in the paravascular endfeet of astrocytes but also at the glia limitans and in juxtaparanodal processes of white matter astrocytes [30, 35]. These juxtaparanodal AQP4 arrays are located immediately adjacent to the myelin sheath of axonal fibers and may be the source of bystander complement responsible for demyelination in vivo. A complement bystander mechanism could explain not only early oligodendrocyte injury and demyelination, as investigated here, but perhaps might also explain in part the early injury to

microvessels in NMO and consequent blood-brain barrier disruption, as brain microvascular endothelial cells are located immediately adjacent to AQP4-enriched endfeet and so may be susceptible to complement bystander injury.

The complement bystander mechanism supported by the data here has implications for NMO therapeutics approaches. Drugs targeting downstream aspects of the inflammatory response may have limited efficacy in preventing oligodendrocyte injury and demyelination in an NMO disease exacerbation if oligodendrocyte injury is produced by a complement bystander mechanism that bypasses the inflammatory response. Similar considerations would apply to other potential complement bystander targets such as microvascular endothelia and corresponding blood-brain barrier disruption. Therapeutics targeting AQP4-IgG levels [31, 32], AQP4-IgG interaction with AQP4 [33, 34], complement, or remyelination [40] would be less affected by a complement bystander mechanism. As formation of the complement membrane attack complex is the major cytotoxic event in bystander killing, drugs targeting late components of complement (C5 through C9), or the complement inhibitor CD59, are predicted to be effective and combinable with drugs targeting alternative mechanisms of NMO pathogenesis.

We note limitations in translating the experimental models data here to human NMO. The rat model necessitated measurements at an early time point following synchronized injection of AQP4-IgG, complement and a dead cell marker, which was necessary to identify injured oligodendrocytes before their disappearance. It would probably by difficult to identify injured oligodendrocytes with MAC deposition in human specimens obtained well after the initiation of NMO pathology and without the aid of a dead cell stain. Another limitation is the differences in densities of astrocytes and oligodendrocytes in human versus rodent brain. Regarding cell coculture models, it is not possible to recapitulate the in vivo AQP4 polarization, inflammatory mechanisms and cellular composition. Our studies focused on mature, myelinating oligodendrocytes rather than immature precursor cells or other CNS cell types. We speculate, however, that complement bystander killing may occur in various other cell types in the CNS that express little CD59 and are in close physical proximity to astrocyte end-feet. We lastly note that although the in vivo rat studies here support a complement bystander mechanism it is difficult to exclude additional local mechanisms that may promote oligodendrocyte injury in vivo such as toxic factors released by injured astrocytes, activated granulocytes [22] or AQP4-specific T cells [4]. A prior study that proposed glutamate-induced oligodendrocyte toxicity following AQP4-IgG-induced astrocyte injury [15], but note that cytotoxicity was minimal and that in vitro coculture data with stagnant extracellular media cannot easily translate to in vivo glutamate toxicity.

In conclusion, our results provide a novel, complement-dependent mechanism in NMO by which AQP4-IgG binding to astrocytes injures surrounding oligodendrocytes, resulting in early and marked demyelination. Our results, however, cannot quantify the relative importance of complement bystander injury verses alternative mechanisms, such as toxins released by injured astrocytes, to early oligodendrocyte injury in human NMO.

## Supplementary Material

Refer to Web version on PubMed Central for supplementary material.

## Acknowledgments

This work was supported by grants EY13574, EB00415, DK35124, and DK72517 from the National Institutes of Health, and a grant from the Guthy-Jackson Charitable Foundation. We thank Dr. Jeffrey Bennett (Univ. Colorado Denver, Aurora, CO) for providing recombinant monoclonal NMO antibody rAb-53.

## References

1. Asavapanumas N, Ratelade J, Verkman AS. Unique neuromyelitis optica pathology produced in naive rats by intracerebral administration of NMO-IgG. Acta Neuropathol. 2014; 127:539–s551. [PubMed: 24190619]
2. Asgari N, Khorooshi R, Lillevang ST, Owens T. Complement-dependent pathogenicity of brain-specific antibodies in cerebrospinal fluid. J Neuroimmunol. 2013; 254:76–82. [PubMed: 23031833]
3. Bennett JL, Lam C, Kalluri SR, Saikali P, Bautista K, Dupree C, Glogowska M, Case D, Antel JP, Owens GP, Gilden D, Nessler S, Stadelmann C, Hemmer B. Intrathecal pathogenic anti-aquaporin-4 antibodies in early neuromyelitis optica. Ann Neurol. 2009; 66:617–629. [PubMed: 19938104]
4. Bradl M, Misu T, Takahashi T, Watanabe M, Mader S, Reindl M, Adzemovic M, Bauer J, Berger T, Fujihara K, Itoyama Y, Lassmann H. Neuromyelitis optica: pathogenicity of patient immunoglobulin in vivo. Ann Neurol. 2009; 66:630–643. [PubMed: 19937948]
5. Brown DR, Krtzschmar HA. The glio-toxic mechanism of α-aminoadipic acid on cultured astrocytes. J Neurocytol. 1998; 27:109–118. [PubMed: 9609401]
6. Crane JM, Lam L, Rossi A, Gupta T, Benett JL, Verkman AS. Binding affinity and specificity of neuromyelitis optica autoantibodies to aquaporin-4 M1/M23 isoforms and orthogonal arrays. J Biol Chem. 2011; 286:16516–16524. [PubMed: 21454592]
7. Dincman TA, Beare JE, Ohri SS, Whittemore SR. Isolation of cortical mouse oligodendrocyte precursor cells. J Neurosci Methods. 2012; 209:219–226. [PubMed: 22743801]
8. Gotze O, Muller-Eberhard HJ. Lysis of erythrocytes by complement in the absence of antibody. J Exp Med. 1970; 132:898–915. [PubMed: 5470509]
9. Hinson SR, Roemer SF, Lucchinetti CF, Fryer JP, Kryzer TJ, Chamberlain JL, Howe CL, Pittock SJ, Lennon VA. Aquaporin-4-binding autoantibodies in patients with neuromyelitis optica impair glutamate transport by down-regulating EAAT2. J Exp Med. 2008; 205:2473–2481. [PubMed: 18838545]
10. Hinson SR, Romero MF, Popescu BF, Lucchinetti CF, Fryer JP, Wolburg H, Fallier-Becher P, Noell S, Lennon VA. Molecular outcomes of neuromyelitis optica (NMO)-IgG binding to aquaporin-4 in astrocytes. Proc Natl Acad Sci USA. 2012; 109:1245–1250. [PubMed: 22128336]
11. Huck S, Grass F, Hortnagl H. The glyamate analog a-aminoadipic acid is taken up by astrocytes before exertingits gliotoxic effect in vitro. J Neurosci. 1984; 4:2650–2657. [PubMed: 6491728]
12. Jarius S, Wildemann B. AQP4 antibodies in neuromyelitis optica: diagnostic and pathogenetic relevance. Nat Rev Neurol. 2010; 6:383–392. [PubMed: 20639914]
13. Lennon VA, Kryzer TJ, Pittock SJ, Verkman AS, Hinson SR. IgG marker of optic-spinal multiple sclerosis binds to the aquaporin-4 water channel. J Exp Med. 2005; 202:473–477. [PubMed: 16087714]
14. Lucchinetti CF, Mandler RN, McGavern D, Bruck W, Gleich G, Ransohoff RM, Trebst C, Weinshenker B, Wingerchuk D, Parisi JE, Lassmann H. A role for humoral mechanisms in the pathogenesis of Devic's neuromyelitis optica. Brain. 2002; 125:1450–1461. [PubMed: 12076996]
15. Marignier R, Nicolle A, Watrin C, Touret M, Cavagna S, Varrin-Doyer M, Cavillon G, Rogemond V, Confavreax C, Honnorat J, Giraudon P. Oligodendrocytes are damages by neuromyelitis optic immunoglobulin G via astrocyte injury. Brain. 2010; 133:2578–2591. [PubMed: 20688809]

16. Misu T, Fujihara K, Kakita A, Konno H, Nakamura M, Watanabe S, Takahashi T, Nakashima I, Takahashi H, Itoyama Y. Loss of aquaporin 4 in lesions of neuromyelitis optica: distinction from multiple sclerosis. Brain. 2007; 130:1224–1234. [PubMed: 17405762]
17. Papadopoulos MC, Verkman AS. Aquaporin 4 and neuromyelitis optica. Lancet Neurol. 2012; 11:535–544. [PubMed: 22608667]
18. Park CC, Shin ML, Simard JM. The complement membrane attack complex and the bystander effect in cerebral vasospasm. J Neurosurg. 1997; 87:294–300. [PubMed: 9254096]
19. Parratt JD, Prineas JW. Neuromyelitis optica: a demyelinating disease characterized by acute destruction and regeneration of a perivascular astrocytes. Mult Scler. 2010; 16:1156–1172. [PubMed: 20823059]
20. Phuan PW, Ratelade J, Rossi A, Tradtrantip L, Verkman AS. Complement-dependent cytotoxicity in neuromyelitis optica requires aquaporin-4 protein assembly in orthogonal arrays. J Biol Chem. 2012; 287:13829–13839. [PubMed: 22393049]
21. Piddleden SJ, Morgan BP. Killing of rat glial cells by complement: deficiency of the rat analogue of CD59 is the cause of oligodendrocyte susceptibility to lysis. J Neuroimmunol. 1993; 48:169–175. [PubMed: 7693753]
22. Ratelade J, Asavapanumas N, Ritchie AM, Wemlinger S, Bennett JL, Verkman AS. Involvement of antibody-dependent cell-mediated cytotoxicity in inflammatory demyelination in a mouse model of neuromyelitis optica. Acta Neuropathol. 2013; 126:699–709. [PubMed: 23995423]
23. Ratelade J, Bennett JL, Verkman AS. Evidence against cellular internalization in vivo of NMO-IgG, aquaporin-4, and excitatory amino acid transporter 2 in neuromyelitis optica. J Biol Chem. 2011; 286:45156–45164. [PubMed: 22069320]
24. Roemer SF, Parisi JE, Lennon VA, Benarroch EE, Lassmann H, Bruck W, Mandler RN, Weinshenker BG, Pittock SJ, Wingerchuk DM, Lucchinetti CF. Pattern-specific loss of aquaporin-4 immunoreactivity distinguishes neuromyelitis optica from multiple sclerosis. Brain. 2007; 130:1194–1205. [PubMed: 17282996]
25. Rossi A, Ratelade J, Papadopoulos MC, Bennett JL, Verkman AS. Neuromyelitis optica (NMO) IgG does not alter aquaporin-4 water permeability, plasma membrane M1/M23 isoform content or supramolecular assembly. Glia. 2012; 60:2027–2039. [PubMed: 22987455]
26. Saadoun S, Waters P, Bell BA, Vincent A, Verkman AS, Papadopoulos MC. Intracerebral injection of neuromyelitis optica immunoglobulin G and human complement produces neuromyelitis optica lesions in mice. Brain. 2010; 133:349–361. [PubMed: 20047900]
27. Sagan SA, Winger RC, Cruz-Herranz A, Nelson PA, Hagberg S, Miller CN, Spencer CM, Ho PP, Bennette JL, Levy M, Levin MH, Verkman AS, Stienman L, Green AJ, Anderson MS, Sobel RA, Zamvil SS. Tolerance checkpoint bypass permits emergence of pathogenic T cells to neuromyelitis optica autoantigen aquaporin-4. Proc Natl Acad Sci USA. 2016; 113:14781–14786. [PubMed: 27940915]
28. Scolding NJ, Morgan BP, Compston DA. The expression of complement regulatory proteins by adult human oligodendrocytes. J Neuroimmunol. 1998; 84:69–75. [PubMed: 9600710]
29. Smith AJ, Jin BJ, Ratelade J, Verkman AS. Aggregation state determines the localization and function of M1- and M23-aquaporin-4 in astrocytes. J Cell Biol. 2014; 204:559–573. [PubMed: 24515349]
30. Smith AJ, Verkman AS. Superresolution imaging of aquaporin-4 cluster size in antibody-stained paraffin brain sections. Biophys J. 2015; 109:2511–2522. [PubMed: 26682810]
31. Tradtrantip L, Asavapanumas N, Verkman AS. Therapeutic cleavage of anti-aquaporin-4 autoantibody in neuromyelitis optica by IgG-selective proteinase. Mol Pharmacol. 2013; 83:1268–1275. [PubMed: 23571414]
32. Tradtrantip L, Ratelade J, Zhang H, Verkman AS. Enzymatic deglycosylation converts pathogenic neuromyelitis optica anti-aquaporin-4 IgG into therapeutic antibody. Ann Neurol. 2011; 73:77–85.
33. Tradtrantip L, Zhang H, Saadoun S, Phuan PW, Lam C, Papadopoulos MC, Bennett JL, Verkman AS. Anti-Aquaporin-4 monoclonal antibody blocker therapy for neuromyelitis optica. Ann Neurol. 2012; 71:314–322. [PubMed: 22271321]

34. Tradtrantip L, Zhang H, Anderson MO, Saadoun S, Phuan PW, Papadopoulos MC, Bennett JL, Verkman AS. Small-molecule inhibitors of NMO-IgG binding to aquaporin-4 reduce astrocyte cytotoxicity in neuromyelitis optica. FASEB J. 2012; 26:2197–2208. [PubMed: 22319008]
35. Waxman SG, Black JA. Freeze-fracture ultrastructure of the perinodal astrocyte and associated glial junctions. Brain Res. 1984; 308:77–87. [PubMed: 6434150]
36. Whitney KD, McNamara JO. GluR3 autoantibodies destroy neural cells in a complement dependent manner modulated by complement regulatory proteins. J Neurosci. 2000; 20:7307–7316. [PubMed: 11007888]
37. Wing MG, Zajicek J, Seilly DJ, Compston DA, Lackmann PI. Oligodendrocytes lack glycolipid anchored proteins which protect them against complement lysis. Restoration of resistence to lysis by incorporation of CD59. Immunology. 1992; 76:140–145. [PubMed: 1378423]
38. Wolburg H, Wolburg-Buchholz K, Fallier-Becker P, Noell S, Mack AF. Structure and functions of aquaporin-4-based orthogonal arrays of particles. Int Rev Cell Mol Biol. 2011; 287:1–41. [PubMed: 21414585]
39. Wrzos C, Winkler A, Metz I, Kayser DM, Thai DR, Wegner C, Bruck W, Nessler S, Bennett JL, Stadelmann C. Early loss of oligodendrocytes in human and experimental neuromyelitis optic lesions. Acta Neuropathol. 2014; 127:523–538. [PubMed: 24292009]
40. Yao X, Su T, Verkman AS. Clobetasol promotes remyelination in a mouse model of neuromyelitis optica. Acta Neuropathol Commun. 2016; 4:42. [PubMed: 27117475]
41. Zipfel PF, Skerka C. Complement regulators and inhibitory proteins. Nat Rev Immunol. 2009; 9:729–740. [PubMed: 19730437]

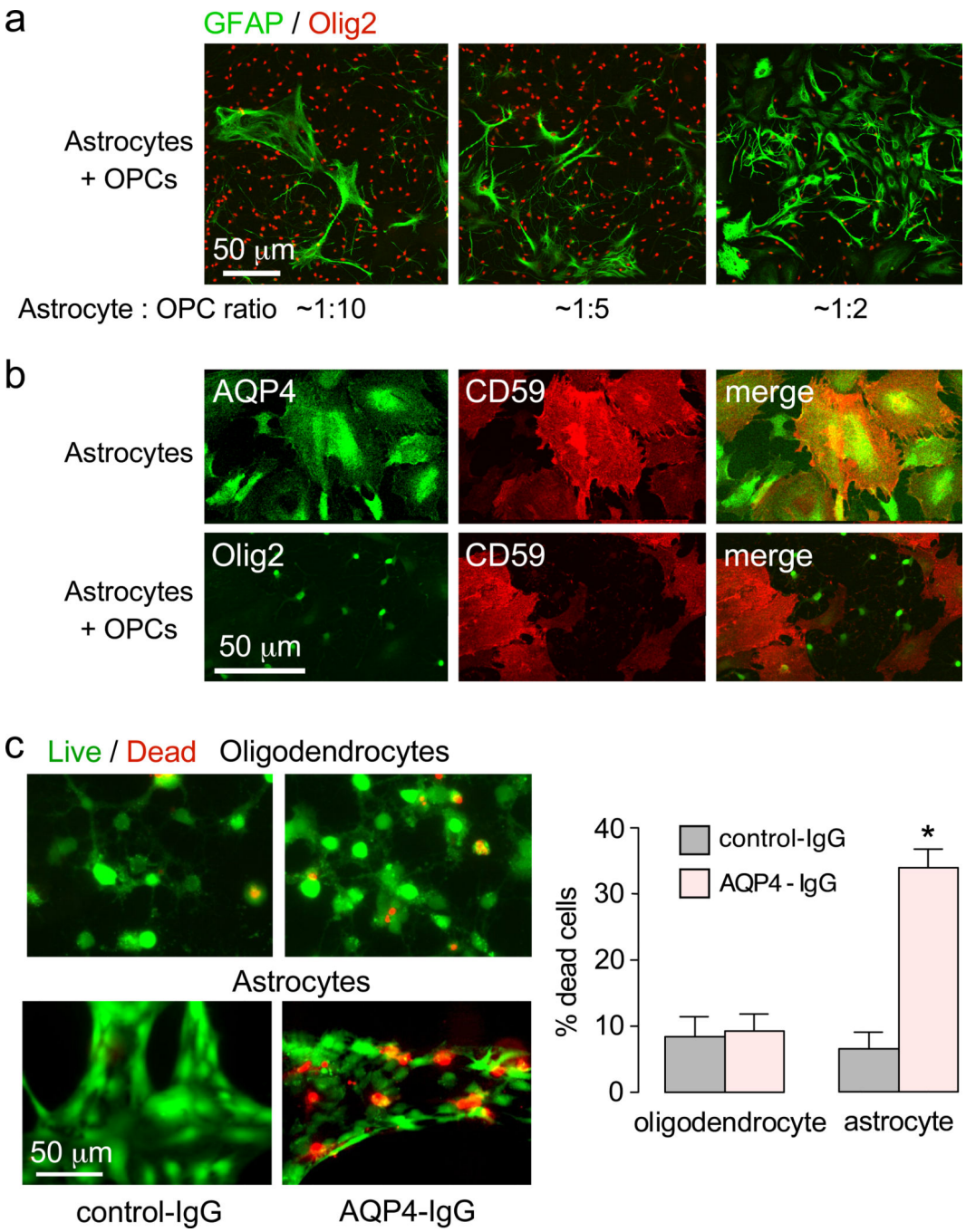


**Figure 1.**

Characterization of rat oligodendrocyte-astrocyte cultures. a. GFAP and Olig2 immunofluorescence of oligodendrocyte-astrocyte cocultures at different cell ratios. Cells were cultured in the presence of 150 ng T3 for 3 days to induce maturation of oligodendrocyte precursor cells. b. AQP4 and CD59 immunofluorescence of astrocyte-oligodendrocyte cocultures. c. Complement-dependent cytotoxicity in pure oligodendrocyte and pure astrocyte cultures, measured by live/dead assay (calcein-AM/ethidium homodimer-1), following 2 h incubation with 30 μg/ml AQP4-IgG and 2% human

complement. Percentage of dead cells summarized at the right (mean ± S.E.M., n=4, * P < 0.01).

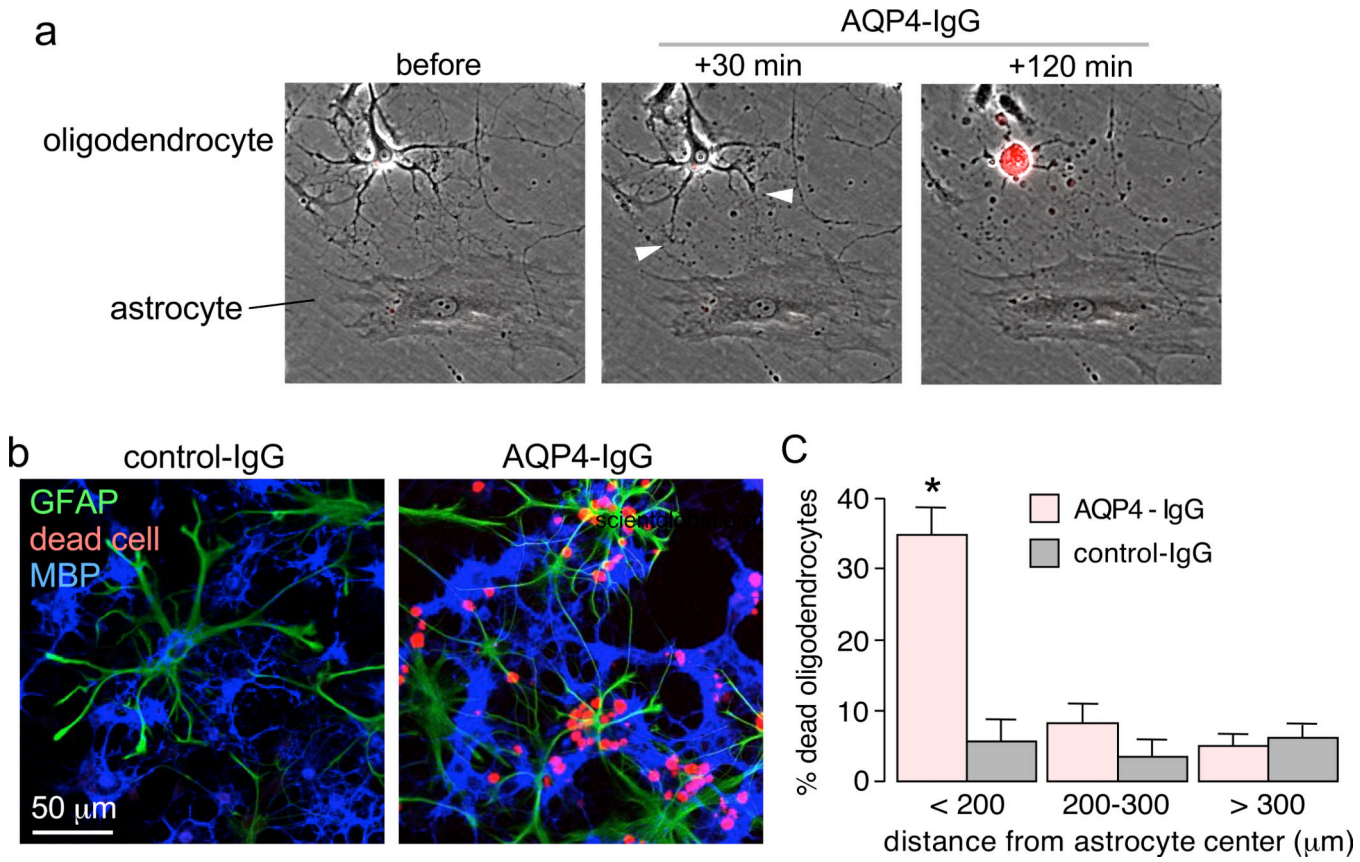


**Figure 2.**

Complement-mediated oligodendrocyte injury in oligodendrocyte-astrocyte cocultures. a. Panels from time-lapse image sequence showing an astrocyte and oligodendrocyte in coculture before and at 30 min and 2 h following addition of 20 μg/ml AQP4-IgG and 2% human complement. Arrowheads point to early retraction of fine oligodendrocyte processes in contact with astrocytes, red color is due to uptake of ethidium homodimer-1 indicating cell death (see Movie 1, Supplemental Data). b. Cocultures incubated as in panel a for 2 hours and immunostained for GFAP and MPB, with red fluorescence seen for a fixable dead cell marker. c. Percentage dead oligodendrocytes at different distances from the center of dead astrocytes (mean ± S.E.M., n=6, * $P < 0.01$ comparing AQP4-IgG vs. control-IgG).

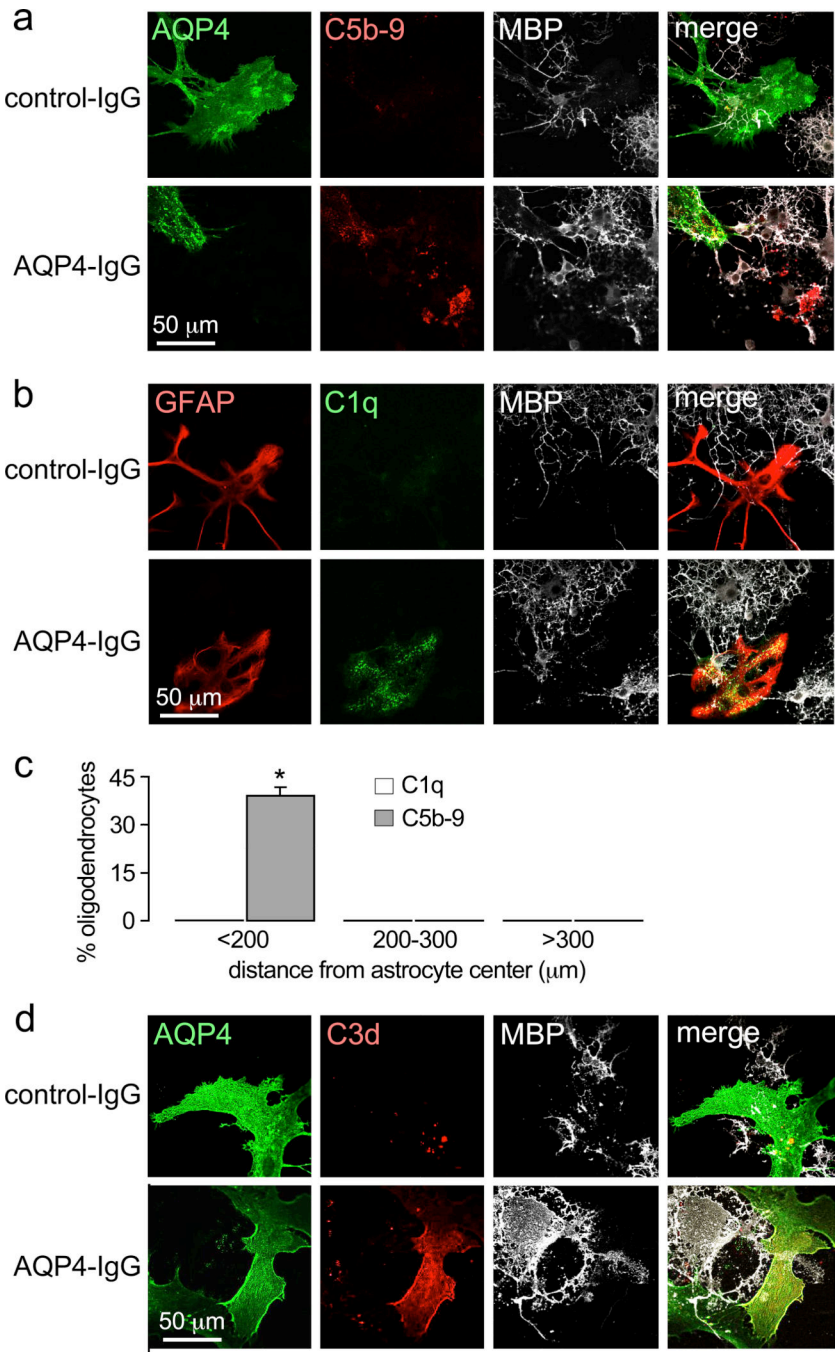


**Figure 3.**

Evidence for a complement bystander mechanism for AQP4-IgG / complement-induced oligodendrocyte injury. C5b-9 (a) and C1q (b) immunofluorescence of astrocyte-oligodendrocyte cocultures at 2 hours after incubation with 20 μg/ml AQP4-IgG and 2% human complement. c. Percentage of C5b-9 and C1q positive oligodendrocytes at different distances from C5b-9 or C1q positive astrocytes (mean ± S.E.M., n=6, * $P < 0.01$ comparing AQP4-IgG vs. control-IgG). d. C3d immunofluorescence of cocultures treated as in panels a and b.

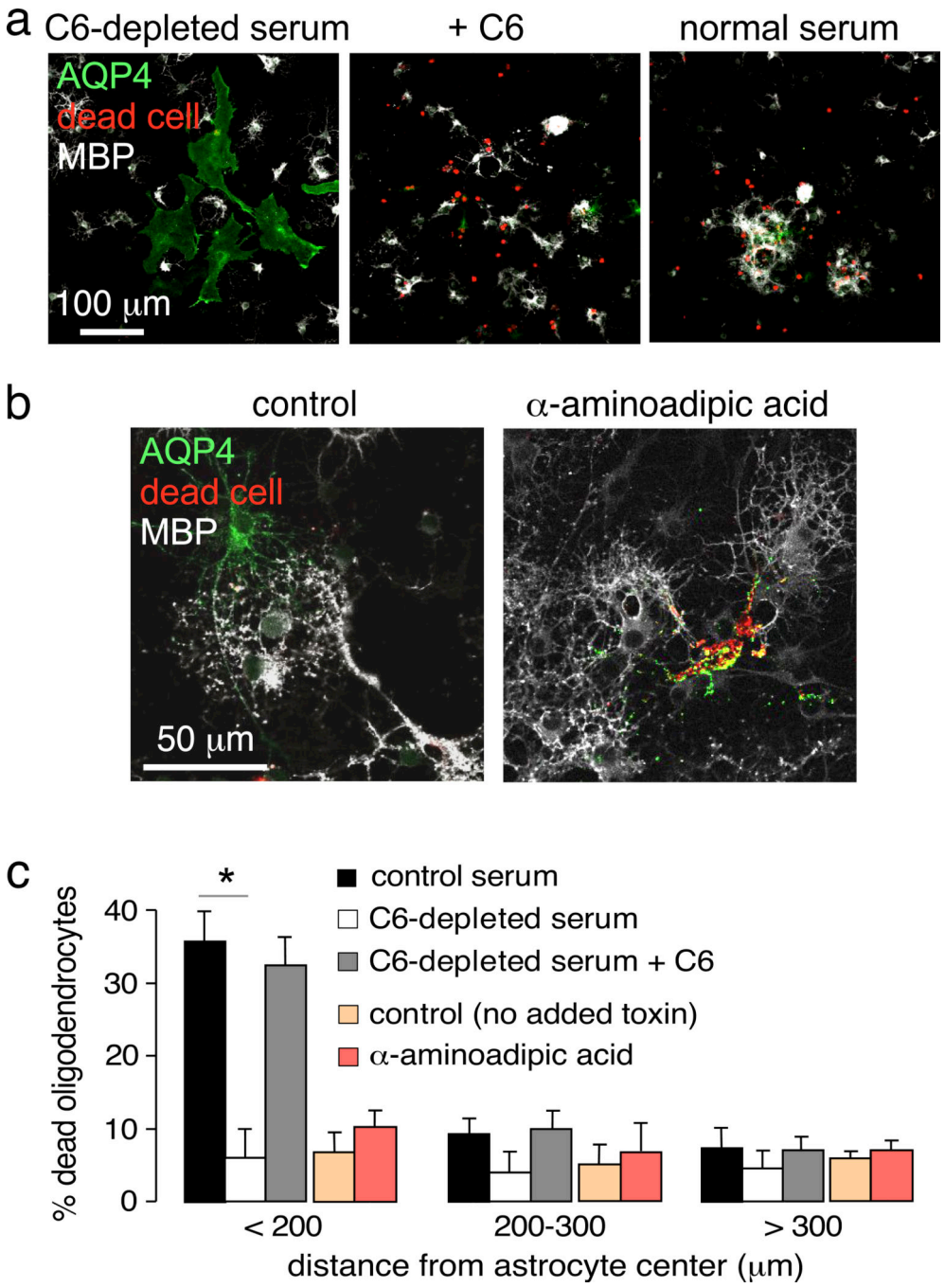


**Figure 4.**

Control studies supporting a complement bystander mechanism. a. Effect of C6 depletion. Cocultures were incubated with 20 μg/ml AQP4-IgG and 2% C6-depleted serum, without or with added C6, immunostained for AQP4 and MBP, with dead cells stained red. b. Direct astrocyte injury by α-aminoadipic acid. Cocultures were exposed to 2 mM α-aminoadipic acid for 75 min and processed as in panel a. c. Percentage dead oligodendrocytes at different distances from the center of dead astrocytes (mean ± S.E.M., n=6, * $P < 0.01$ comparing with control serum for each distance range).

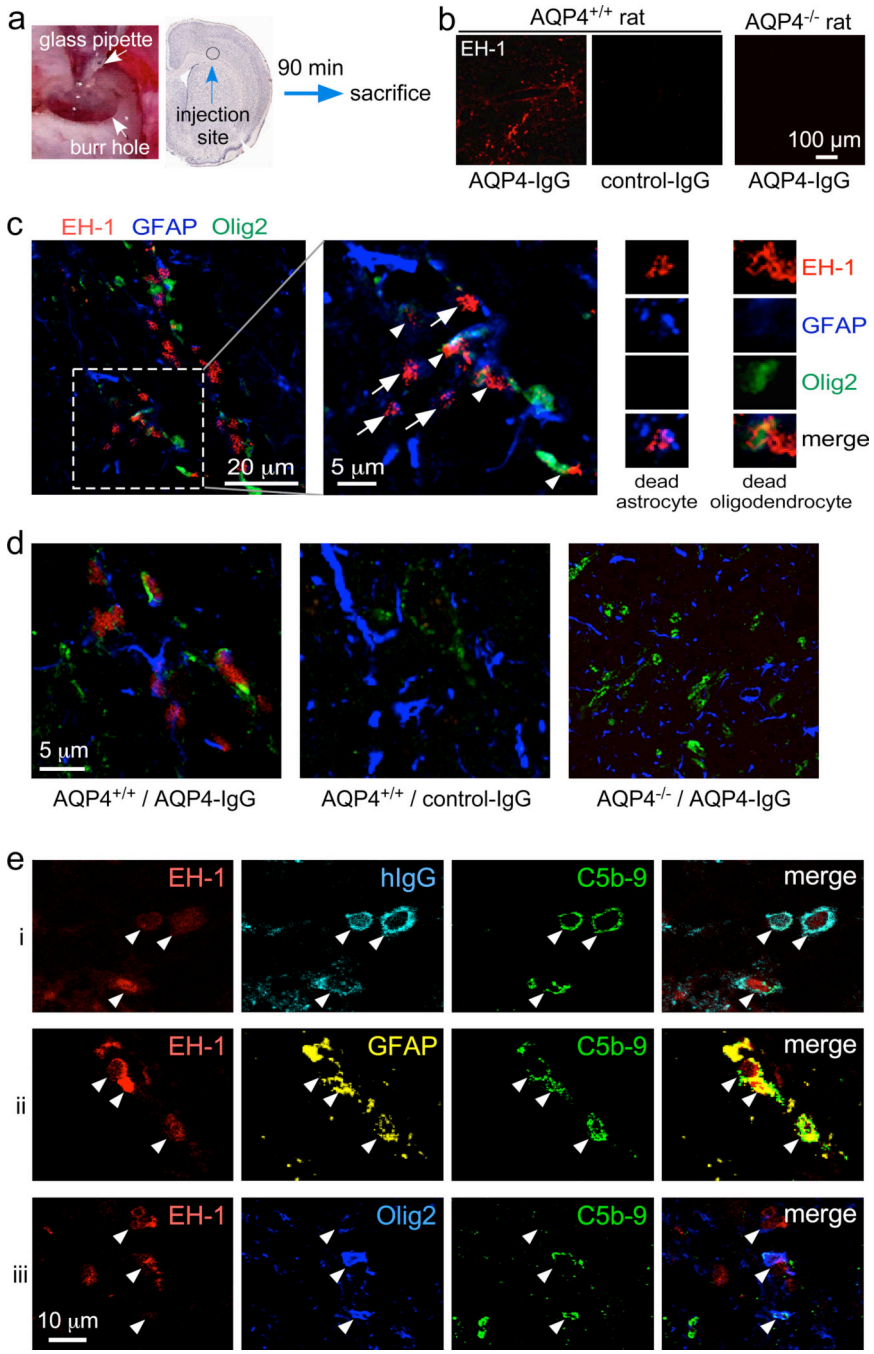


**Figure 5.**

Evidence for complement bystander mechanism for AQP4-IgG-induced oligodendrocyte injury in rat brain. a. AQP4-IgG (15 μg) (or control human IgG), human complement (26%) and fixable dead cell dye ethidium homodimer-1 (EH-1) (6 μM) in a 6-μl volume was injected in cortex and striatum of rat brain and rat were sacrificed at 90 min. b. Low-magnification micrographs showing dead cells (red EH-1 fluorescence) for studies done in $AQP4^{+/+}$ and $AQP4^{-/-}$ rats. c. High-magnification confocal images of $AQP4^{+/+}$ rat brain 90 min after injection of AQP4-IgG, complement and EH-1, showing dead astrocytes (white

arrows) and nearby injured oligodendrocytes (white arrowheads). Expanded images on the right show dead (EH-1 positive) astrocyte and oligodendrocyte. d. Images as in panel c (center) showing representative fields from brains of $AQP4^{+/+}$ and $AQP4^{-/-}$ rats following AQP4-IgG or control IgG injection. e. High-magnification confocal micrographs of brain from AQP4-IgG-injected $AQP4^{+/+}$ rat showing colocalization (white arrowheads) of EH-1, hIgG and C5b-9 (row i), EH-1, GFAP and C5b-9 (row ii), and EH-1, Olig2 and C5b-9 (row iii).

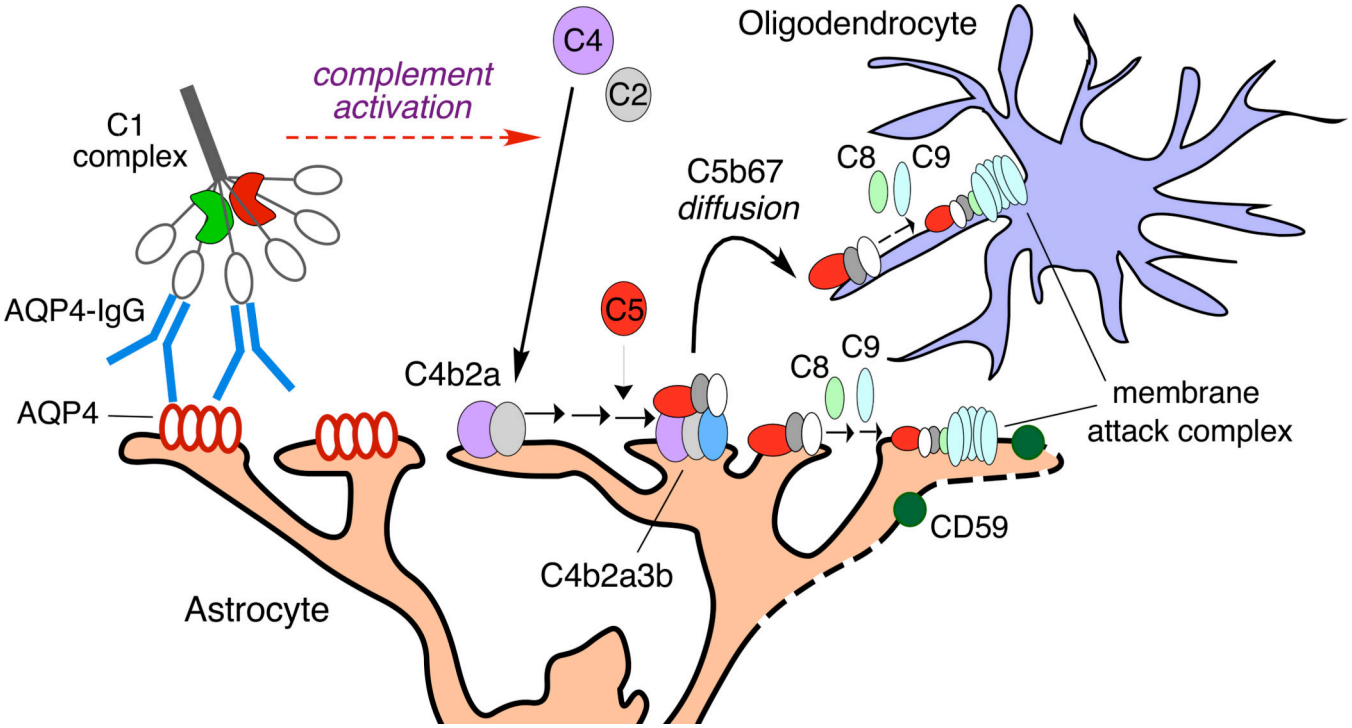


**Figure 6.**

Proposed bystander mechanism for complement-dependent oligodendrocyte injury following AQP4-IgG binding to AQP4 on astrocytes. Bystander injury results from diffusion of the C5b67 complement complex from astrocytes to nearby oligodendrocytes. See text for explanations.